Computer Methods and Programs in Biomedicine 148 (2017) 91–98

Contents lists available at ScienceDirect

Computer Methods and Programs in Biomedicine

journal homepage: www.elsevier.com/locate/cmpb

Computational modeling for prediction of the shear stress of three-dimensional isotropic and aligned fiber networks

Seungman Park

Department of Mechanical Engineering, Johns Hopkins University, Baltimore, MD, USA

ARTICLE INFO

Article history:
Received 4 February 2017
Revised 17 June 2017
Accepted 26 June 2017

Keywords:
Interstitial flow (IF)
Extracellular matrix (ECM)
Permeability
Average shear stress (ASS)
Computational modeling

ABSTRACT

Background and objective: Interstitial flow (IF) is a creeping flow through the interstitial space of the extracellular matrix (ECM). IF plays a key role in diverse biological functions, such as tissue homeostasis, cell function and behavior. Currently, most studies that have characterized IF have focused on the permeability of ECM or shear stress distribution on the cells, but less is known about the prediction of shear stress on the individual fibers or fiber networks despite its significance in the alignment of matrix fibers and cells observed in fibrotic or wound tissues. In this study, I developed a computational model to predict shear stress for different structured fibrous networks.

Methods: To generate isotropic models, a random growth algorithm and a second-order orientation tensor were employed. Then, a three-dimensional (3D) solid model was created using computer-aided design (CAD) software for the aligned models (i.e., parallel, perpendicular and cubic models). Subsequently, a tetrahedral unstructured mesh was generated and flow solutions were calculated by solving equations for mass and momentum conservation for all models. Through the flow solutions, I estimated permeability using Darcy's law. Average shear stress (ASS) on the fibers was calculated by averaging the wall shear stress of the fibers. By using nonlinear surface fitting of permeability, viscosity, velocity, porosity and ASS, I devised new computational models.

Results: Overall, the developed models showed that higher porosity induced higher permeability, as previous empirical and theoretical models have shown. For comparison of the permeability, the present computational models were matched well with previous models, which justify our computational approach. ASS tended to increase linearly with respect to inlet velocity and dynamic viscosity, whereas permeability was almost the same. Finally, the developed model nicely predicted the ASS values that had been directly estimated from computational fluid dynamics (CFD).

Conclusions: The present computational models will provide new tools for predicting accurate functional properties and designing fibrous porous materials, thereby significantly advancing tissue engineering.

1. Introduction

Interstitial flow (IF) is a creeping flow through the interstitial space of the extracellular matrix (ECM) [1]. IF has been known to play a key role in maintaining tissue homeostasis by transporting cytokines, antigens, nutrients, and various signaling molecules, which have a significant effect on various functions of cells and tissues such as cell differentiation, growth, and tissue remodeling [2–4]. It also plays a morphoregulator to form blood or lymphatic vessels and induces mechanical strain to align the collagen matrix [5–7].

To characterize the IF, the hydraulic permeability (or Darcy's permeability), k, has been widely used, which is dependent on porosity (ϕ), or solid volume fraction ($1-\phi$), fiber diameter, and network orientation [8–10]. Until now, numerous studies have demonstrated that permeability increased with increasing porosity [11,12], and fiber arrays perpendicular to the fluid flow decreased the permeability compared with arrays parallel to the fluid flow [13]. In addition, permeability was rapidly increased in the tissue swelling caused by inflammation or tissue injury [14].

Shear force or stress exerted on the fiber can be another way to characterize the interstitial flow; it is generated by the fluid phase passing through the ECM. However, most studies to characterize IF have focused on the permeability as a flow resistance parameter [15,16] or shear stress distribution on the cells, but less is known about the prediction of shear stress on the fibers despite its significance associated with the alignment of matrix fibers and cells observed in fibrotic or wound tissues [17]. Yao et al. investigated the effect of IF on the shear stress distribution on the mast cell through a three-dimensional (3D) computational model [18]. Ped-

E-mail address: smpark138@gmail.com

http://dx.doi.org/10.1016/j.cmpb.2017.06.019
0169-2607/

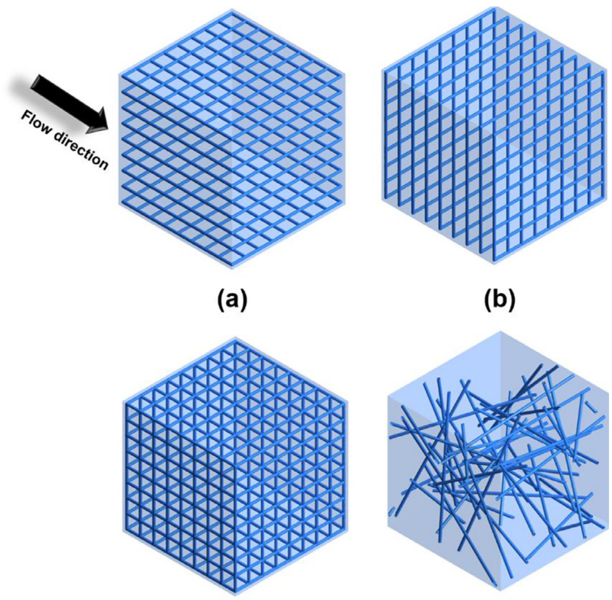

Fig. 1. Examples of the fibrous microstructures considered in this study: (a) parallel, (b) perpendicular, (c) cubic, and (d) isotropic model. The fiber radius is 500 nm and box size is $50 \times 50 \times 50\,\mu m^3$. (For interpretation of the references to color in this figure legend, the reader is referred to the web version of this article.)

ersen et al. showed that ECM architecture and orientation can affect shear stress distribution on a cell [13,19]. Wang and Tarbell [20] developed a predictive model to estimate average shear stress (ASS), τ, on spherical cells in a 3D matrix using the Brinkman equation as follows:

$$\tau_{cell} \cong \frac{\mu V_{if}}{k^{0.5}}, \quad (1)$$

where μ is the dynamic viscosity and V_{if} is interstitial fluid velocity.

However, most of these models were designed for a simplified shaped cell, such as a sphere, and do not consider the effect of real complex matrix architecture, which is known to significantly affect IF. Motivated by this fact, I developed a 3D computational model to predict ASS on the fiber to answer the following questions: (1) How does the matrix architecture or fiber orientation affect the ASS on the ECM fiber? (2) How does the porosity or solid volume fraction influence ASS? First, permeability was calculated based on the flow solutions through the computational fluid dynamics (CFD) approach and compared with previous empirical and theoretical models to validate our model developed in this study. Second, the effect of the dynamic viscosity and velocity on the permeability and shear stress on the fiber was examined. Third, the effect of porosity or fiber volume fraction on the shear stress was investigated. On the basis of porosity and shear stress, new predictive models for ASS were introduced.

2. Materials and methods

2. 1. Construction of the fibrous matrices

Four different types of fiber networks were created: parallel and perpendicular to the flow, cubic, and isotropic model (Fig. 1). Details for dimensions of parallel, perpendicular, and cubic models [Fig. 1(a)–(c)] have been described elsewhere [13].

For the isotropic model [Fig. 1(d)], a random growth algorithm was employed as reported elsewhere [8]. In brief, nucleation points were randomly formed with the uniform distribution within the cubic space [Fig. 2(a)]. Each point grew independently along a randomly chosen unit vector in opposite directions [Fig. 2(b)]. The fiber growth stopped when they collided with the cubic boundary surfaces [Fig. 2(c)]. The fluid box size is $50 \times 50 \times 50\ \mu m^3$. The fibers are assumed to be fixed at a box surface, which means that fibers do not move due to the interstitial flow. When two fibers collide, they are designed to be merged.

For the characterization of isotropic models, the second-order orientation tensor (Ω) was utilized as follows [21]:

$$\Omega = \frac{1}{l_{tot}} \sum l_i \times \begin{bmatrix} \sin^2\alpha_i \cos^2\vartheta_i & \sin^2\alpha_i \sin\vartheta_i \cos\vartheta_i & \cos\alpha_i \sin\alpha_i \cos\vartheta_i \\ \sin^2\alpha_i \sin\vartheta_i \cos\vartheta_i & \sin^2\alpha_i \sin^2\vartheta_i & \cos\alpha_i \sin\alpha_i \sin\vartheta_i \\ \cos\alpha_i \sin\alpha_i \cos\vartheta_i & \cos\alpha_i \sin\alpha_i \sin\vartheta_i & \cos^2\alpha_i \end{bmatrix}, \quad (2)$$

where l_i is the length of the *ith* fiber and l_{tot} is the total fiber length. α is the elevation angle, which is formed by the fiber axis and the z axis. ϑ is the azimuth angle, which is formed between the projection of the fiber on the x–y plane and the x axis. For the isotropic case, on-diagonal components Ω_{xx}, Ω_{yy}, and Ω_{zz} have a similar value as approximately 1/3, and the trace of Ω is always 1.

Table 1 presents a summary of parameters of generated models. The radius considered in the models ranged from 250 to 1500 nm depending on the model type, and the corresponding porosity varied from 0.814 to 0.991. For the isotropic model, two numbers (30 and 50) for the generation of nucleation points were used. Diagonal components (Ω_{xx}, Ω_{yy}, and Ω_{zz}), which are a measure of fiber alignment in the coordinate direction, showed a value close to 0.333 for both 30 and 50 of fibers. Permeability was highly associated with fiber radius, porosity, and fiber alignment. First, the parallel model to the fluid flow showed higher permeability ($1.97\,\mu m^2$) than the perpendicular model ($0.93\,\mu m^2$) under the same fiber radius and porosity. Under the same fiber radius (500, 1000, and 1500 nm) for the two isotropic models (30 and 50), higher porosity generated higher permeability.

2.2. Computational methods: assumptions, boundary conditions, meshing, and simulation

Fig. 3 shows a flow chart from the computational modeling to analysis. Briefly, generated data for the construction of fiber networks were converted into surface and solid models through SolidWorks (SolidWorks 2016) [Fig. 3(a)]. Tetrahedral mesh on the solid model was created using ICEM-CFD (ANSYS 14.5), and finer mesh was applied as closer to the fiber curvature [Fig. 3(b)]. This is because the fiber surface is assumed as the non-slip condition, there is high velocity gradient as closer to the fiber surface. Thus, to precisely describe the velocity field, more mesh with smaller sizes should be used. To make sure that results should not be affected by the number of mesh, grid sensitivity test was carried out. For each model, 10 different numbers of mesh were tested (Fig. 4). The higher number of mesh tends to be proportional to the accuracy but requires more time for calculation. Thus, the simulation was performed with the gradually increasing number of mesh. As a result, there was a region showing small variation among data (as shown in blue dashed line, Fig. 4). These values were utilized as the representative shear stress value for each model. Additionally, the higher the porosity, the more mesh is required. Since models with the lower diameter have a higher porosity, these models have higher numbers of mesh than ones with a higher diameter. Hence, depending on the size and complexity of fibrous networks, 1,000,000–8,000,000 elements were generated in the simulations. Finally, computational analysis was performed after solving gov-